



# CHORUS

This is the accepted manuscript made available via CHORUS. The article has been published as:

## Quasisymmetric Optimization of Nonaxisymmetry in Tokamaks

J.-K. Park, S. M. Yang, N. C. Logan, Q. Hu, C. Zhu, M. C. Zarnstorff, R. Nazikian, C. Paz-Soldan, Y. M. Jeon, and W. H. Ko

Phys. Rev. Lett. **126**, 125001 — Published 26 March 2021

DOI: [10.1103/PhysRevLett.126.125001](https://doi.org/10.1103/PhysRevLett.126.125001)

# Quasi-symmetric optimization of non-axisymmetry in tokamaks

J.-K. Park,<sup>1,\*</sup> S. M. Yang,<sup>1</sup> N. C. Logan,<sup>1</sup> Q. Hu,<sup>1</sup> C. Zhu,<sup>1</sup> M. C. Zarnstorff,<sup>1</sup>  
C. Paz-Soldan,<sup>2</sup> Y. M. Jeon,<sup>3</sup> and W. H. Ko<sup>3</sup>

<sup>1</sup>*Princeton Plasma Physics Laboratory, Princeton, New jersey 08543, USA*

<sup>2</sup>*General Atomics, San Diego, California, USA*

<sup>3</sup>*National Fusion Research Institute, Daejeon 305-333, Republic of Korea*

(Dated: December 2, 2020)

Predictive 3D optimization reveals a novel approach to modify a non-axisymmetric magnetic perturbation to be entirely harmless for tokamaks, by essentially restoring quasi-symmetry in perturbed particle orbits as much as possible. Such a quasi-symmetric magnetic perturbation (QSMP) has been designed and successfully tested in the KSTAR and DIII-D tokamaks, demonstrating no performance degradation despite the large overall amplitudes of non-axisymmetric fields and strong response otherwise expected in the tested plasmas. The results indicate that a quasi-symmetric optimization is a robust path of error field correction across the resonant and non-resonant field spectrum in a tokamak, leveraging the prevailing concept of quasi-symmetry for general toroidal 3D plasmas such as stellarators. The optimization becomes, in fact, a simple eigenvalue problem to the so-called torque response matrices if a perturbed equilibrium is calculated consistent with non-axisymmetric neoclassical transport.

PACS numbers:

Magnetic fusion strongly relies on a symmetry in the magnetic field to confine hot and charged particles inside a vessel. It is the toroidal axisymmetry in a tokamak that fundamentally offers good thermal plasma confinement within toroidal magnetic surfaces [1, 2], while also providing engineering simplicity. Nonetheless, the axisymmetry can never be perfect in reality and a small non-axisymmetric error field must be under control as otherwise it can induce unnecessary transport effects such as the toroidal drag of rotating plasmas. The immediate proof of the value of error field control in tokamaks is to increase the propensity of the plasma to rotate toroidally, which helps the disruption avoidance [3–9] and eases transition to or sustainment of high confinement modes [10–13]. This becomes more important as tokamaks grow in size, since the relative amount of torque that can be applied externally decreases [14]. If the error field can not be reduced in magnitudes by correcting field, an ideal alternative is to modify the non-axisymmetry into a symmetry required to conserve the action of particles on magnetic surfaces [15, 16] and thereby preserve original confinement as much as possible. This paper reports the first design and experimental demonstration of such a quasi-symmetric magnetic perturbation in tokamaks, which illuminates a reliable path of comprehensive error field correction in fusion burning plasmas [17].

Small non-axisymmetry  $\delta\vec{B}$  in the tokamak magnetic field  $\vec{B}_0 = B_0\hat{b}$  can still conserve the action of particles  $\mathcal{J} = \oint v_{\parallel} dl$ , the integral of the parallel velocity  $v_{\parallel}$  along the trajectories  $dl$ , if the field strength along the field lines remains unchanged, i.e.  $|(\vec{B}_0 + \delta\vec{B})(\vec{x} + \vec{\xi})| = |\vec{B}_0(\vec{x})|$ . The displacement of the field lines  $\vec{\xi}$  moves plasmas almost ideally through Faraday's and Ohm's laws, giving the condition for quasi-symmetry in a perturbed tokamak

[18] as

$$\delta_{\mathcal{L}} \equiv \left( \hat{b} \cdot \vec{\nabla} \vec{\xi} \cdot \hat{b} - \vec{\nabla} \cdot \vec{\xi} \right) \sim 0, \quad (1)$$

to the leading order in particular on the so-called Boozer coordinates [19]. This condition is however not compatible with the perturbed plasma equilibrium  $\delta\vec{F}[\vec{\xi}] = 0$  [20] that dictates the  $\vec{\xi}$  profiles and thus can not be satisfied globally across the plasma, as is known generally for 3D magnetic confinement systems [21]. This is also true for the omnigenity [22, 23]  $\delta\mathcal{J} \sim 0$  which is less constrained in average than  $\delta_{\mathcal{L}} \sim 0$ .

The best practice for minimizing the deviation from this symmetry is offered by integrating the calculations of perturbed equilibria into the prediction of its final consequences to confinement, which can be represented by the toroidal drag force  $T_{\varphi}(\psi) = \text{Im}[n \int^{\psi} d\vec{x}(\vec{\xi} \cdot \delta\vec{F})]$  [18]. The torque  $T_{\varphi}$  inside a torus at the radial label  $\psi$  is due to  $\delta\vec{j} \times \delta\vec{B}$  with the non-ambipolar current  $\delta\vec{j}$  associated with particles radially drifting off magnetic surfaces to conserve the action  $\mathcal{J}$  when  $\delta_{\mathcal{L}} \neq 0$  [24]. The torque density  $\tau_{\varphi}(\psi) = dT_{\varphi}/dV$  with the volume of the torus  $V$  by a species with the charge  $q$  becomes the direct measure of the additional particle flux  $\Gamma$  due to the non-axisymmetry, by  $\Gamma = q\tau_{\varphi}$ . Note that a perturbation is described with the complex Fourier representation  $\propto e^{i(m\vartheta - n\varphi)}$  with the  $m$  poloidal and  $n$  toroidal mode along the two angles  $(\vartheta, \varphi)$ . The unique product of such a self-consistent formulation, implemented in general perturbed equilibrium code (GPEC) [25], is the torque response matrix function  $\overleftrightarrow{\mathcal{T}}(\psi)$  in the Fourier space, which simplifies the problem of quasi-symmetric optimization into a matrix exercise by

$$T_{\varphi}(\psi) = \vec{\Phi}^{\dagger} \cdot \overleftrightarrow{\mathcal{T}}(\psi) \cdot \vec{\Phi} = \vec{C}^{\dagger} \cdot \overleftrightarrow{\mathcal{T}}_C(\psi) \cdot \vec{C} \sim 0. \quad (2)$$

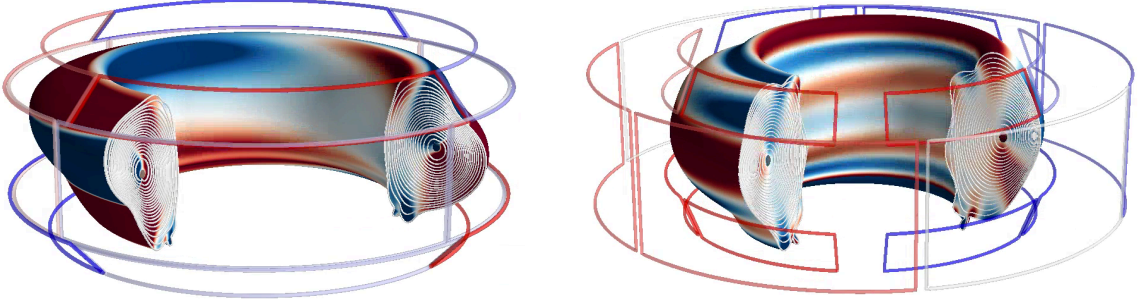


FIG. 1: Quasi-symmetric  $n = 1$  configurations tested in the KSTAR (left) #22972 and the DIII-D (right) #178620 high- $\beta$  tokamak plasmas using their 3 rows of versatile control coils, with the perturbed flux surfaces (amplified visually by  $\times 25$  for KSTAR and  $\times 10$  for DIII-D), and the illustrated distribution of non-axisymmetric magnetic fields and coil currents in colors (in red for + and blue for - with contrast proportional to their amplitudes.)

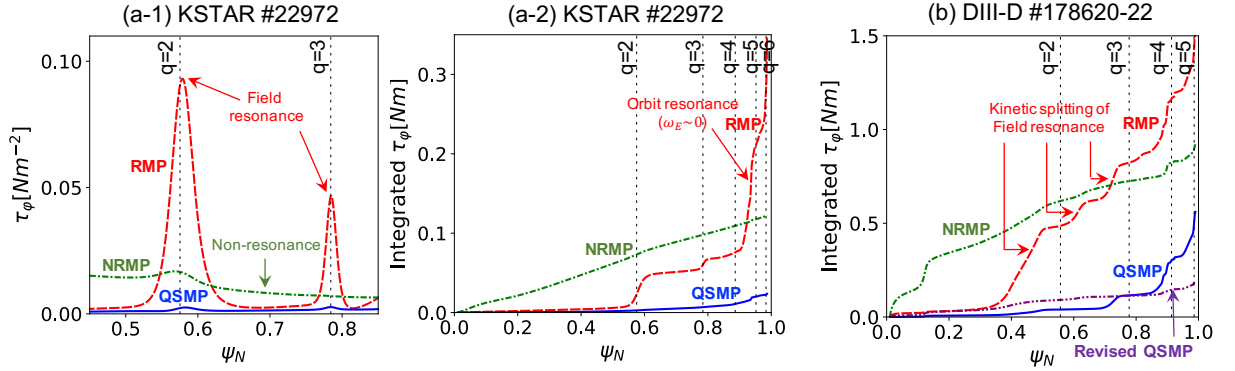


FIG. 2: Comparison of the (a-1) predicted torque density, (a-2) integrated torque profiles in the KSTAR and (b) DIII-D discharges by QSMPs (blue), NRMPs (green) and RMPs (red). The RMP produces torque mainly through the field resonances, whereas the NRMP induces torque and transport broadly across the region. The QSMP optimization leads to the suppression of both effects as well as the kinetic orbit-resonant effect, as pronounced in the (a-2) RMP application. In very high- $\beta$  plasmas like the studied DIII-D case, the field resonance is shifted and split due to the kinetic effects which can strongly change the originally optimized spectrum as implied by the revisited QSMP (light-blue).

The matrix  $\vec{T}$  can be represented on any basis set as long as it uniquely represents non-axisymmetric magnetic perturbations available in space. For example,  $\vec{\Phi}$  is the perturbed magnetic flux decomposed to Fourier modes on the plasma boundary, and  $\vec{C}$  is the amplitude and phase of currents in available non-axisymmetric coils. Since  $\vec{T}^\dagger = \vec{T}$  [25], its eigenvector  $\vec{C}_{min}$  with the minimum eigenvalue  $\lambda_{min}$  is simply the best achievable quasi-symmetric magnetic perturbation (QSMP) in a tokamak, as illustrated in Fig. 1 and successfully demonstrated in the two tokamak devices - KSTAR [26] and DIII-D [27].

These two devices were particularly suitable for this test since they both have versatile 3D coils that can generate 3 distinct perturbed field distributions in arbitrary phase for  $n = 1$ , which tends to be most amplified by plasma response [28] and thus can magnify the potentially small transport effects driven by QSMPs. Both devices have small uncertainties in non-axisymmetric machine errors, either due to an intrinsically low level [29] or with an established correction algorithm [8]. For each

target plasma,  $\vec{T}_C(\psi)$  is a mere  $3 \times 3$  complex matrix function but still has all the information of the toroidal torque that can be produced by the coils for the given  $n$ . Figure 1 shows the perturbed flux surfaces and field distributions in the KSTAR and DIII-D target plasmas, with the coil configurations and perturbations designed using  $\vec{C}_{min}$  from the GPEC  $\vec{T}_C(\psi = \psi_b)$  where  $\psi_b$  is the numerical plasma boundary, i.e., minimizing the total integrated torque down to the theoretical minimum  $\lambda_{min}$ .

QSMPs were then contrasted to the other two distinct types of non-axisymmetric fields - a resonant magnetic perturbation (RMP) [30] and non-resonant magnetic perturbation (NRMP) [31], as introduced in Fig. 2 with each of the predicted torque profiles. As clearly shown in Fig. 2 (a-1), the RMP strongly resonates with the plasmas at the rational surfaces  $q = m/n$ , where the safety factor  $q$  is the ratio of toroidal to poloidal circuits of the magnetic field lines, with locally concentrated torque density making the stair-like jumps in the integrated torque, Fig.

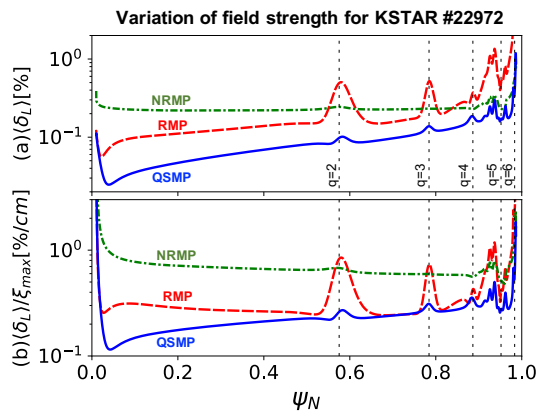


FIG. 3: Comparison of the (a) field strength averaged on magnetic surfaces (up) and the (b) same but normalized by overall response (down), by the QSMP, NRMP, and RMP applied to the KSTAR discharge. Note that here the RMP and NRMP have the same  $|\vec{C}|$ , i.e., the *rms* sum of 3 rows of coil currents, whereas the QSMP is based on a higher  $|\vec{C}|$  up to the maximum allowed in the experiments.

2 (a-2) and (b). The NRMPs' effect is widely spread throughout the entire region, resulting in a gradual and smooth increase of the integrated torque from the core to the edge. This classification is important for practical purposes. The goal of the RMP optimization is to create a local resonant response without NRMP effects to control instabilities such as edge-localized-modes (ELMs) [32–38], whereas the goal of the NRMP optimization is to purposely create the torque to control the rotation profile [31, 39–42] in a particular region but without RMP response. Note that the RMP response includes not only the toroidal drag, or rotational damping, but also a bifurcation into magnetic islands due to the local toroidal torque which can consequently lead to other transport effects such as density pumping [43] or disruptive instabilities such as a locked mode [3]. A QSMP suppresses both effects, requiring at least 3 rows of coils like KSTAR or DIII-D for a successful demonstration - one coil to produce a strong proxy error, another coil to minimize the RMP and yet another to further minimize the NRMP components. An ultimate goal of 3D tokamak optimization would be to leave only QSMPs everywhere except a region where the applied RMP or NRMP is judiciously designed to take an effect for the control purposes.

The optimization of various non-axisymmetric fields becomes comprehensive only with a kinetic calculation integrated into perturbed equilibria. As indicated in Fig. 2 (a-2), the QSMP also minimizes the orbit-resonant effect which becomes strong when  $\vec{E} \times \vec{B}$  rotation  $\omega_E$  is low, i.e.  $\omega_E \sim 0$  or more generally for any particle that cycles to a closed orbit by  $(\ell \pm nq)\omega_b + n(\omega_E + \omega_B) \sim 0$  where  $\omega_b$  is the bounce frequency and  $\omega_B$  is the magnetic precession frequency with an integer  $\ell$  [44]. In high-

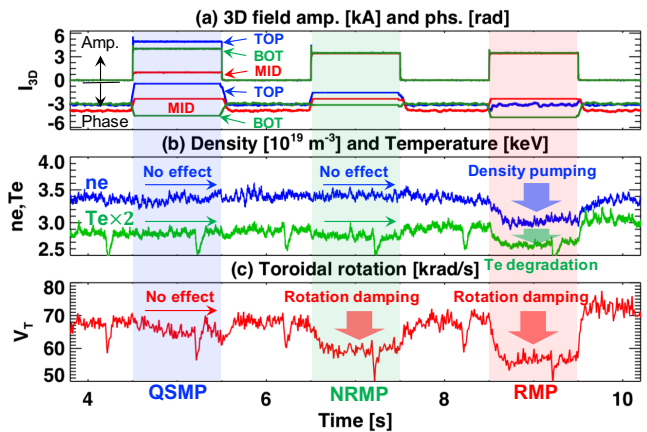


FIG. 4: Impact of QSMP, NRMP, and RMP shown by the time traces in a single dedicated KSTAR discharge; (a) 3D coil configurations with 3 amplitudes and phases (rad) for top, middle, bottom row of in-vessel coils, (b)  $\bar{n}_e$  measured by two-color interferometer (TCI) and  $T_e$  measured by electron-cyclotron emission (ECE) at  $R \sim 1.98m$ , and (c)  $\omega_\varphi$  measured by charge-exchange recombination spectroscopy (CERS) at  $R \sim 2.0m$ .

performance scenarios like the studied DIII-D cases, the field resonance  $m - nq = 0$  is also largely shifted and split due to local kinetic effects as indicated in Fig. 2 (b) by stair-like jumps in both sides to the rational surface. The orbital kinetics is then combined with perturbed equilibria where the amplitude and distribution of  $\vec{\xi}$  are simultaneously optimized in a QSMP, as illustrated in Fig. 3 for the KSTAR case. Figure 3 (a) in comparison to (b) implies the importance of the reduction of overall plasma response as roughly represented by  $\xi_{max}$  at each surface. The strong plasma response to a small 3D field makes it challenging to intuitively understand the QSMP optimizing process in a tokamak, requiring extended investigations in the future.

These model predictions have been validated then by the measured transport in experimental KSTAR and DIII-D discharges. The KSTAR discharge was assisted by neutral beam injection (NBI) with heating power  $P_{nb} \sim 3MW$  and estimated torque  $T_{nb} \sim 2.9Nm$ , operating the plasma current  $I_P = 0.5MA$ , the toroidal field at the magnetic axis  $B_{T0} = 1.8T$ , which produced  $\beta_N \sim 1.8$ , normalized thermal to magnetic pressure [45], and a safety factor at  $\psi = 0.95$ ,  $q_{95} \sim 5$ , line-averaged density  $\bar{n}_e \sim 3.4 \times 10^{19}m^{-3}$ , ion and electron temperature  $T_i \sim 2.2keV$  and  $T_e \sim 2.3keV$ , and toroidal rotation  $\omega_\varphi \sim 100krad/s$  at the core. Figure 4 shows time traces of the  $n = 1$  field amplitudes and phases in 3 rows of coils (Top, Middle, Bottom coils),  $\bar{n}_e$ ,  $T_e$  and  $\omega_\varphi$  slightly off the center at  $R \sim 2m$ . The RMP induced perturbations in all transport channels of particle, energy and momentum as is clear by density pumping, temperature degradation, and rotational damping, while the NRMP

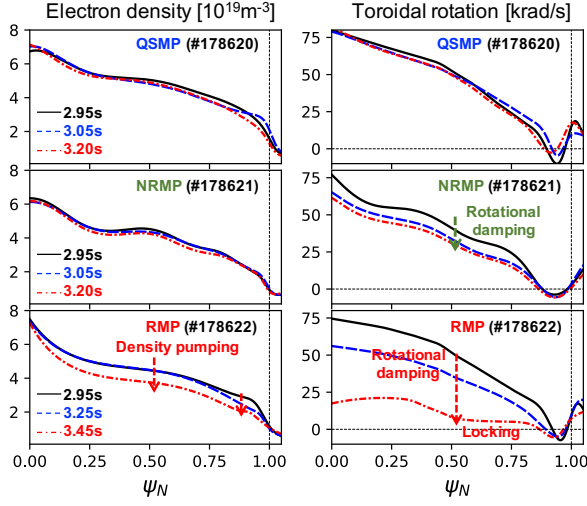


FIG. 5: Impact of QSMP, NRMP, and RMP fields on the  $n_e$  and  $\omega_\phi$  profiles as measured before (solid in black) and after (dash in blue, and dashed-dot in red) the perturbations. Note that the QSMP or NRMP was ramped to its desired maximum at  $t = 3.05s$  but RMP was slowly ramped until it caused a locking and disruption. Note the profiles were taken from OMFIT profile toolkit [47].

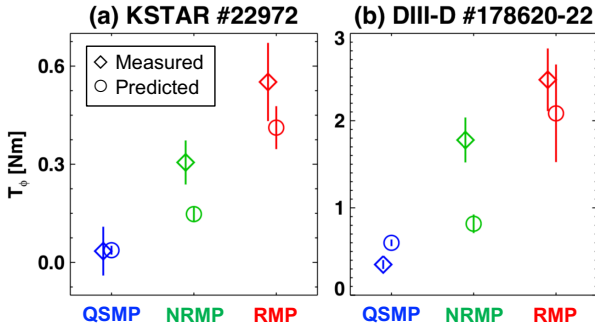


FIG. 6: Comparison of the predicted and measured total torques by QSMP, NRMP, RMP in the (a) KSTAR and (b) DIII-D discharges.

induced only rotational damping. In contrast, the QSMP did not bring any visible effect, despite the maximum KSTAR 3D coil currents up to  $\sim 5kA$ .

The benign nature of QSMP was also clearly evinced in DIII-D, compared with NRMP or RMP. The DIII-D experiment targeted high-performance discharges to have a plasma very sensitive to residual non-axisymmetric fields through the well-known increase of plasma amplification along with  $\beta_N$  [28, 46]. The co-NBIs up to  $P_{nb} \sim 8.5MW$  on  $I_P = 1.2MA$ ,  $B_{T0} = 1.8T$  injected torque  $T_{nb} \sim 6.7Nm$  and increased  $\beta_N > 3.0$  with  $q_{95} = 4.3$ ,  $\bar{n}_e \sim 5.0 \times 10^{19}m^{-3}$ ,  $T_i \sim 6keV$ ,  $T_e \sim 4.3keV$ , and  $\omega_\phi \sim 80krad/s$  at the core of the target discharges. Figure 5 shows the density and rotation profile changes due to QSMP, NRMP, and RMP in the DIII-D plasmas.

Again, the plasma was strongly degraded in all channels and eventually disrupted with a locked mode by the RMP, degraded in rotation by the NRMP, but not influenced in any way by the QSMP despite the maximum coil currents.

The predictive optimization by GPEC torque response matrix has also been validated quantitatively as far as the total integrated torque is concerned, as shown in Fig. 6. The predictions here include uncertainties in calculating non-trapped (passing) particle effects, in addition to trapped particle effects which have been extensively verified [44, 48]. The torque measurements are simply based on the changes of total angular momentum  $L$  of the plasmas, using the mean of  $T_\phi = T_{NBI} \times (\Delta L/L)$  and  $T_\phi = dL/dt$  with error bars used to show the deviation between the two methods. These methods ignore momentum transport across the region, which is largely uncertain but can be critical in the future to validate the predicted torque density with rotational damping profiles in detail.

Robustness of the QSMP optimization is also noticeable. Coil configuration optimizations performed well despite non-exact reproduction of the reference discharge used in the predictive modeling. For example, the DIII-D QSMP was designed based on a  $\beta_N \sim 2.0$  plasma (#173383) and applied to the high- $\beta_N > 3.0$  (#178620-22), but did not show any degradation in experiments. The difference in the prediction from the re-optimized QSMP for the new target is not entirely ignorable as shown by 'QSMP rev.' in Fig. 2 (b), but mainly through the edge profiles which are subjected to relatively low accuracy. The same QSMP configuration was even applied to a plasma during the L-H transition [49] with marginal power  $P_{nb} \sim 1MW$  and  $T_{nb} \sim 0.83Nm$  (#178609-10) and did not show any impact on the transition. This target was disrupted by a NRMP, similarly to the recent observations in the COMPASS tokamak where large NRMPs were left due to high-field-side non-axisymmetric error fields compensated by low-field-side RMP correction [50].

A practical implication of these observations for the error field correction (EFC) problem is that the QSMP indeed encapsulates an ideal and safe form of non-axisymmetry. An EFC coil configuration containing a fixed EF source in  $\vec{C}$  can be optimized as quasi-symmetric as this will simultaneously minimize the negative impact of both the resonant and resonant EF components. The quality of the non-resonant correction can then be quantitatively measured by GPEC torque response matrix. The torque response matrices  $\vec{T}$  with respect to the full poloidal modes  $\vec{\Phi}$  on the boundary, as shown in Fig. 7, typify the second mode group with  $m < nq$  which is mostly non-resonant but still degrading, in addition to the primary mode group with  $m > nq$  which is typically known as the dominant Kink modes [6, 46, 51]. These components of the EF would naturally be controlled in

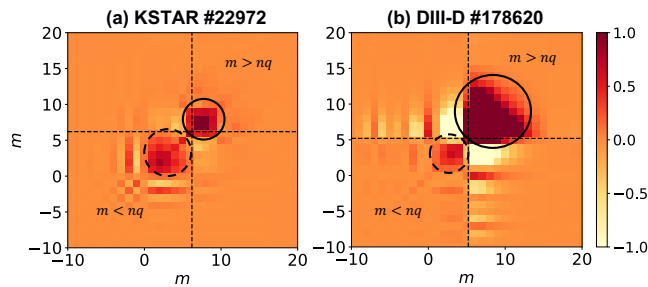


FIG. 7: Structure of the integrated torque response matrix  $\vec{T}$  calculated at the plasma boundary for the (a) KSTAR ( $10^{-3} Nm/G^2$ ) and (b) DIII-D ( $10^{-2} Nm/G^2$ ) plasmas. The solid circle indicates the dominant mode group with  $m > nq$ , and the second circle represents the second non-resonant mode group with  $m < nq$ .

addition to the resonant components when using a QSMP optimization scheme for EFC.

In summary, new GPEC predictive schemes enabled the first design and demonstration of quasi-symmetric magnetic perturbations in tokamaks. Both KSTAR and DIII-D experiments show quiescence of QSMPs in all transport channels despite the large amplitude of perturbations, rendering a group of safe non-axisymmetric fields. The studies illuminate the feasibility of prevailing concept of quasi-symmetry even in a perturbed tokamak, and also a robust path of comprehensive error field correction. It is not yet clear if there is any utility of QSMPs for a tokamak, e.g. heat flux distributions to the divertors, or if 3D stability also remains unchanged, which should be further investigated in the future.

## ACKNOWLEDGMENT

The authors would like to thank T. Markovic in the Institute of Plasma Physics of the Czech Academy of Sciences for having us updated on recent COMPASS experiments which imply the importance of non-resonant error field correction in a tokamak.

This material is based upon work supported by the U.S. Department of Energy, Office of Science, Office of Fusion Energy Sciences, using the DIII-D National Fusion Facility, a DOE Office of Science user facility, under Award(s) DE-AC02-09CH11466 (Princeton Plasmas Physics Laboratory), DE-FC02-04ER54698 (DIII-D), DE-SC0020298 (Collaborative Research in Magnetic Fusion Energy Sciences on International Tokamaks, General Atomics), and also by the Korean Ministry of Science, ICT and Future Planning (KSTAR).

DISCLAIMER: This report was prepared as an account of work sponsored by an agency of the United States Government. Neither the United States Government nor any agency thereof, nor any of their employees,

makes any warranty, express or implied, or assumes any legal liability or responsibility for the accuracy, completeness, or usefulness of any information, apparatus, product, or process disclosed, or represents that its use would not infringe privately owned rights. Reference herein to any specific commercial product, process, or service by trade name, trademark, manufacturer, or otherwise does not necessarily constitute or imply its endorsement, recommendation, or favoring by the United States Government or any agency thereof. The views and opinions of authors expressed herein do not necessarily state or reflect those of the United States Government or any agency thereof.

\* Electronic address: [jpark@pppl.gov](mailto:jpark@pppl.gov)

- [1] A. H. Boozer, Plasma Phys. Control. Fusion **50**, 124005 (2008).
- [2] P. Helander, C. D. Beidler, T. M. Bird, M. Drevlak, Y. Feng, R. Hatzky, F. Jenko, R. Kleiber, J. H. E. Proll, Y. Turkin, et al., Plasma Phys. Control. Fusion **54**, 124009 (2012).
- [3] R. Fitzpatrick and T. C. Hender, Phys. Fluids B **3**, 644 (1991).
- [4] R. J. La Haye, R. Fitzpatrick, T. C. Hender, A. W. Morris, J. T. Scoville, and T. N. Todd, Phys. Fluids B **4**, 2098 (1992).
- [5] R. J. Buttery, M. D. Benedetti, D. A. Gates, Y. Gribov, T. Hender, R. J. La Haye, P. Leahy, J. A. Leuer, A. W. Morris, A. Santagiustina, et al., Nucl. Fusion **39**, 1827 (1999).
- [6] J.-K. Park, M. J. Schaffer, J. E. Menard, and A. H. Boozer, Phys. Rev. Lett. **99**, 195003 (2007).
- [7] J. E. Menard, R. E. Bell, D. A. Gates, S. P. Gerhardt, J.-K. Park, S. A. Sabbagh, J. W. Berkery, A. Egan, J. Kallman, S. M. Kaye, et al., Nucl. Fusion **50**, 045008 (2010).
- [8] C. Paz-Soldan, M. J. Lanctot, N. C. Logan, D. Shiraki, R. J. Buttery, J. M. Hanson, R. J. L. Haye, J.-K. Park, W. M. Solomon, and E. J. Strait, Phys. Plasmas **21**, 072503 (2014).
- [9] Y. In, J.-K. Park, Y. M. Jeon, J. Kim, G. Y. Park, J.-W. Ahn, A. Loarte, W. H. Ko, H. H. Lee, J. W. Yoo, et al., Nucl. Fusion **57**, 116054 (2017).
- [10] P. Gohil, G. R. McKee, D. Schlossberg, L. Schmitz, and G. Wang, J. Phys. Conf. Ser. **123**, 021017 (2008).
- [11] S. P. Gerhardt, J. E. Menard, J.-K. Park, R. Bell, D. A. Gates, B. P. LeBlanc, S. A. Sabbagh, and H. Yuh, Plasma Phys. Control. Fusion **52**, 104003 (2010).
- [12] Y. Sun, Y. Liang, H. R. Koslowski, S. Jachmich, A. Alfier, O. Asunta, G. Corrigan, C. Giroud, M. P. Gryaznevich, D. Harting, et al., Plasma Phys. Control. Fusion **52**, 105007 (2010).
- [13] C. Paz-Soldan, N. C. Logan, M. J. Lanctot, J. M. Hanson, J. D. King, R. J. L. Haye, R. Nazikian, J.-K. Park, and E. J. Strait, Nucl. Fusion **55**, 083012 (2015).
- [14] C. Chrystal, B. A. Grierson, G. M. Staebler, C. C. Petty, W. M. Solomon, J. S. deGrassie, K. H. Burrell, T. Tala, and A. Salmi, Phys. Plasmas **24**, 056113 (2017).
- [15] C. Nüenberg and R. Zille, Phys. Lett. A **129**, 113 (1988).
- [16] A. H. Boozer, Plasma Phys. Control. Fusion **37**, A103

- (1995).
- [17] K. Ikeda, Nucl. Fusion **47**, S1 (2007).
- [18] J.-K. Park, Phys. Plasmas **18**, 110702 (2011).
- [19] A. H. Boozer, Phys. Fluids **24**, 1999 (1981).
- [20] A. H. Boozer and C. Nührenberg, Phys. Plasmas **13**, 102501 (2006).
- [21] D. A. Garren and A. H. Boozer, Phys. Fluids B **3**, 2822 (1991).
- [22] J. R. Cary and S. G. Shasharina, Phys. Rev. Lett. **78**, 674 (1997).
- [23] M. Landreman and P. J. Catto, Phys. Plasmas **19**, 056103 (2012).
- [24] J.-K. Park, A. H. Boozer, and J. E. Menard, Phys. Rev. Lett. **102**, 065002 (2009).
- [25] J.-K. Park and N. C. Logan, Phys. Plasmas **24**, 032505 (2017).
- [26] G. S. Lee et al., Nucl. Fusion **40**, 575 (2000).
- [27] J. L. Luxon and L. G. Davis, Fusion Technology **8**, 441 (1985).
- [28] A. H. Boozer, Phys. Rev. Lett. **86**, 5059 (2001).
- [29] Y. In, J.-K. Park, J. M. Jeon, J. Kim, and M. Okabayashi, Nucl. Fusion **55**, 043004 (2015).
- [30] T. E. Evans, R. A. Moyer, P. R. Thomas, J. G. Watkins, T. H. Osborne, J. A. Boedo, E. J. Doyle, M. E. Fenstermacher, K. H. Finken, R. J. Groebner, et al., Phys. Rev. Lett. **92**, 235003 (2004).
- [31] J.-K. Park, Y. M. Jeon, J. E. Menard, W. H. Ko, S. G. Lee, Y. S. Bae, M. Joung, K.-I. You, K.-D. Lee, N. C. Logan, et al., Phys. Rev. Lett. **111**, 095002 (2013).
- [32] T. Evans, M. Fenstermacher, A. Moyer, T. Osborne, J.G.Watkins, P. Gohil, I. Joseph, M. Schaffer, L. Baylor, M. Bécoulet, et al., Nucl. Fusion **48**, 024002 (2008).
- [33] Y. Liang, H. R. Koslowski, P. R. Thomas, E. Nardon, B. Alper, P. Andrew, Y. Andrew, G. Arnoux, Y. Baranov, M. Bécoulet, et al., Phys. Rev. Lett. **98**, 265004 (2007).
- [34] W. Suttrop, T. Eich, J. C. Fuchs, S. Gunter, A. Janzer, A. Herrmann, A. Kallenbach, P. T. Lang, T. Lunt, M. Maraschek, et al., Phys. Rev. Lett. **106**, 225004 (2011).
- [35] A. Kirk, J. Harrison, Y. Liu, E. Nardon, I. T. Chapman, P. Denner, and the MAST Team, Phys. Rev. Lett. **108**, 255003 (2012).
- [36] Y. M. Jeon et al., Phys. Rev. Lett. **109**, 035004 (2012).
- [37] R. Nazikian, C. Paz-Soldan, J. D. Callen, J. S. deGrassie, D. Eldon, T. E. Evans, N. M. Ferraro, B. A. Grierson, R. J. Groebner, S. R. Haskey, et al., Phys. Rev. Lett. **114**, 105002 (2015).
- [38] Y. Sun, Y. Liang, Y. Q. Liu, S. Gu, X. Yang, W. Guo, T. Shi, M. Jia, L. Wang, B. Lyu, et al., Phys. Rev. Lett. **117**, 115001 (2016).
- [39] K. H. Burrell, A. M. Garofalo, W. M. Solomon, M. E. Fenstermacher, T. H. Osborne, J.-K. Park, M. J. Schaffer, and P. B. Snyder, Phys. Plasmas **19**, 056117 (2012).
- [40] K. Kim, W. Choe, Y. In, W. H. Ko, M. J. Choi, J. G. Bak, H. S. Kim, Y. M. Jeon, and J. G. Kwak, Nucl. Fusion **57**, 126035 (2017).
- [41] Y. In, Y. M. Jeon, J.-K. Park, A. Loarte, J.-W. Ahn, J. H. Lee, H. H. Lee, G. Y. Park, K. Kim, et al., Nucl. Fusion **59**, 056009 (2019).
- [42] S. M. Yang, J.-K. Park, Y.-S. Na, Z. Wang, W. H. Ko, Y. In, J. H. Lee, K. D. Lee, and S. K. Kim, Phys. Rev. Lett. **123**, 095001 (2019).
- [43] Q. Hu, R. Nazikian, B. A. Grierson, N. C. Logan, J.-K. Park, C. Paz-Soldan, and Q. Yu, Phys. Plasmas **26**, 120702 (2019).
- [44] N. C. Logan, J.-K. Park, K. Kim, Z. R. Wang, and J. W. Berkery, Plasma Phys. **20**, 122507 (2013).
- [45] F. Troyon, R. Gruber, H. Saurenmann, S. Semenzato, and S. Succi, Plasma Phys. Control. Fusion **26**, 209 (1984).
- [46] M. J. Lanctot, H. Reimerdes, A. M. Garofalo, M. S. Chu, Y. Q. Liu, E. J. Strait, G. L. Jackson, R. J. La Haye, M. Okabayashi, T. H. Osborne, et al., Phys. Plasmas **17**, 030701 (2010).
- [47] N. C. Logan, B. A. Grierson, S. R. Haskey, S. P. Smith, O. Meneghini, and D. Eldon, Fusion Sci. Technol. **74**, 125 (2018).
- [48] Z. Wang, J.-K. Park, Y. Liu, N. Logan, K. Kim, and J. E. Menard, Phys. Plasmas **21**, 042502 (2014).
- [49] F. Wagner, G. Fussmann, T. Grave, M. Keilhacker, M. Kornherr, K. Lackner, K. McCormick, E. R. Muller, A. Stabler, G. Becker, et al., Phys. Rev. Lett. **53**, 1453 (1984).
- [50] T. Markovic, M. Peterka, A. Loarte, J.-K. Park, Y. Gribov, J. Havlicek, R. Panek, P. Hacek, M. Hron, M. Imrisek, et al., <http://ohhttp://ocs.ciemat.es/EPS2018ABS/pdf/03.108.pdf> (2018), in Proceedings of the 45th EPS Conference.
- [51] H. Reimerdes, A. M. Garofalo, E. J. Strait, R. J. Buttery, M. S. Chu, Y. In, G. L. Jackson, R. J. La Haye, R. J. Lanctot, Y. Q. Liu, et al., Nucl. Fusion **49**, 115001 (2009).